Modulation of Induced Gamma Band Responses in a Perceptual Learning Task in the Human EEG

Thomas Gruber[1], Matthias M. Müller[1], and Andreas Keil[2]

Abstract

■ Fragmented pictures of an object, which appear meaningless when seen for the first time, can easily be identified after the presentation of an unfragmented version of the same picture. The neuronal mechanism for such a rapid perceptual learning phenomenon is largely unknown. Recently, induced gamma band responses (GBRs) have been discussed as a possible physiological correlate of activity in cell assemblies formed by learning. The present study was designed to investigate the modulation of induced GBRs in a perceptual learning task by using a 128-channel EEG montage. In the first sequence of the experiment, fragmented pictures from the Snodgrass and Vandervart inventory were presented. The fragmentation of the pictures was selected that subjects were unable to identify them. In the second experimental sequence—the perceptual learning sequence—half of the pictures were displayed in their unfragmented version. In the third sequence, all pictures were presented again in the fragmented version. Now, subjects had to rate whether or not they could identify the images. Results showed an increase in spectral gamma power at parietal electrode sites for identified pictures. In addition, neural activity in the gamma band was highly synchronized between posterior electrodes. For pictures not presented in their complete version, we found no such pattern in the third sequence. From our results, we concluded that induced GBRs might represent a signature of synchronized neural activity in a Hebbian cell assembly, activated by the fragmented picture after perceptual learning took place. No difference between identified and unidentified pictures was found in the visual evoked potential in the same time range and in the evoked GBR in the same frequency range as the induced response. ■

INTRODUCTION

A fragmented picture of an object, which appears meaningless when seen for the first time, can easily be identified after the presentation of the unfragmented version of the same picture (Ramachandran, 1994). This process, known as rapid perceptual learning, that is, the facilitation in the identification of fragmented pictures after prior exposure, has been described first by Leeper (1935). However, the mechanism underlying this form of object identification is still under discussion. In general, it has been suggested that sensory input is matched against memory representations. In different theories, these representations have been described as ''geons'' (Biederman, 1987), prototypes or ''pictogens'' (Humphrey & Bruce, 1989; Warren & Morton, 1982), or as a match between object tokens and their representation in memory (Treisman, 1992). However, (1) the nature of sensory representations in memory, (2) the contribution of bottom-up versus top-down processes, (3) the time course of their interaction, and (4) the involvement of implicit and explicit memory systems are still under discussion (Viggiano & Kutas, 2000; Schacter, Bowers, & Booker, 1989). In order to unravel these puzzles, Schacter (1992) suggested a cognitive neuroscience perspective to understand the underlying brain mechanisms. Neuroscientific findings suggest that information about different features of an object seems not to be processed in a single cortical area. Rather, multiple visual areas are involved (Tootell, Dale, Sereno, & Malach, 1996; Zeki, 1993; Felleman & van Essen, 1991). With respect to the visual system, it was suggested that distinct regions of information processing remain segregated throughout higher areas in the brain and can be divided into two streams of information processing (Tootell et al., 1996; Zeki, 1993; Livingstone & Hubel, 1988). The ventral pathway is thought to be specialized for the analysis of object features like color, shape, and so forth, while the dorsal pathway seems to be specialized for the analysis of motion and spatial relationship between objects (Ungerleider & Haxby, 1994; Ungerleider, 1995; Roland, Gulyas, Seitz, Bohm, & Stone-Elander, 1990). Furthermore, object knowledge seems to be stored in a distributed neural network in which information about specific features is stored close to the regions of the cortex that mediates the perception of those features (Ungerleider, 1995; Roland et al., 1990). Thus, in a rapid perceptual learning task using fragmented pictures one might expect that the learned features of an object are stored in visual areas of both pathways (Martin, Haxby, Lalonde, Wiggs, & Ungerleider, 1995), because shape and spatial

[1]University of Liverpool, UK, [2]University of Konstanz, Germany

relationships between fragments have to be processed (Treisman, 1988). Given these assumptions, the question arises as to the mechanism that integrates the neuronal activity within and between the elements of such a network. Theoretical considerations and intracortical recordings in animals suggested that synchronized bursts of action potentials in a frequency range above 20 Hz, that is, the gamma band, is a signature of such a mechanism (Singer & Gray, 1995; Hummel & Biederman, 1992; Eckhorn, Reitboeck, Arndt, & Dicke, 1990; Singer et al., 1990; Gray, König, Engel, & Singer, 1989; Gray, Engel, König, & Singer, 1990; Malsburg & Schneider, 1986; Milner, 1974). These synchronized oscillations are neither phase nor time locked to stimulus onset, thus being called induced gamma band responses (GBRs) as opposed to stimulus locked evoked responses, like the visual evoked potential (VEP) or the evoked GBR.

In a series of studies, it has been shown that induced GBRs in the human EEG are related to visual information processing (Keil, Müller, Ray, Gruber, & Elbert, 1999; Rodriguez et al., 1999; Tallon-Baudry, Bertrand, Delpuech, & Pernier, 1997; Tallon-Baudry, Bertrand, Wienbruch, Ross, & Pantev, 1997; Müller et al., 1996; Müller, Junghöfer, Elbert, & Rockstroh, 1997; Lutzenberger, Pulvermüller, Elbert, & Birbaumer, 1995) and are modulated not only by the feature of a stimulus but also by visual-spatial attention (Müller, Gruber, & Keil, 2000; Müller & Gruber, 2001; Gruber, Müller, Keil, & Elbert, 1999). One common finding in all EEG studies is a latency of induced GBRs between 200 and 400 msec after stimulus onset. Evoked GBRs, on the other hand, occur with a latency of about 100 msec after stimulus onset (Herrmann, Mecklinger, & Pfeifer, 1999; Tallon, Bertrand, Bouchet, & Pernier, 1995), but the significance of evoked GBRs is still not clear. The long latency of induced GBRs is in variance with early visual information processing where one would expect latencies between 50 and 80 msec (Gomez-Gonzales, Clark, Fan, Luck, & Hillyard, 1994). Therefore, induced GBRs in the human EEG are discussed as being (1) a signature of bottom-up and top-down attentional feature processing (Müller et al., 2000; Müller & Gruber, 2001; Tallon-Baudry & Bertrand, 1999), (2) related to short-term memory (Tallon-Baudry, Bertrand, Peronnet, & Pernier, 1998), and (3) induced by learned cognitive representations of a stimulus (Gruber, Keil, & Müller, 2001; Pulvermüller, 1996). Obviously, the different proposals are not mutually exclusive. The relation of induced GBRs to Hebbian cell assemblies is common to all proposals. Such cell assemblies are formed on the simple rule: ''Cells that fire together wire together'' (Hebb, 1949). Recently, it has been discussed that gamma power alone is an insufficient marker for synchronous neural activity between different cortical areas (Lachaux, Rodriguez, Martinerie, & Varela, 1999; Miltner, Braun, Arnold, Witte, & Taub, 1999; Rodriguez et al., 1999). These authors suggested that phase synchrony between pairs of electrodes, independent of amplitude, provides a better measure for integrative activity in a cell assembly. The build-up of such a cell assembly can be investigated in learning paradigms. In a conditioning paradigm, Miltner et al. (1999) showed not only an increase in gamma power at electrodes over different cortical areas but also, and this is even more important, a significant phase coherency. This phase coherency was seen as an empirical evidence of synchronized neural activity across distant cortical areas. Similar results were

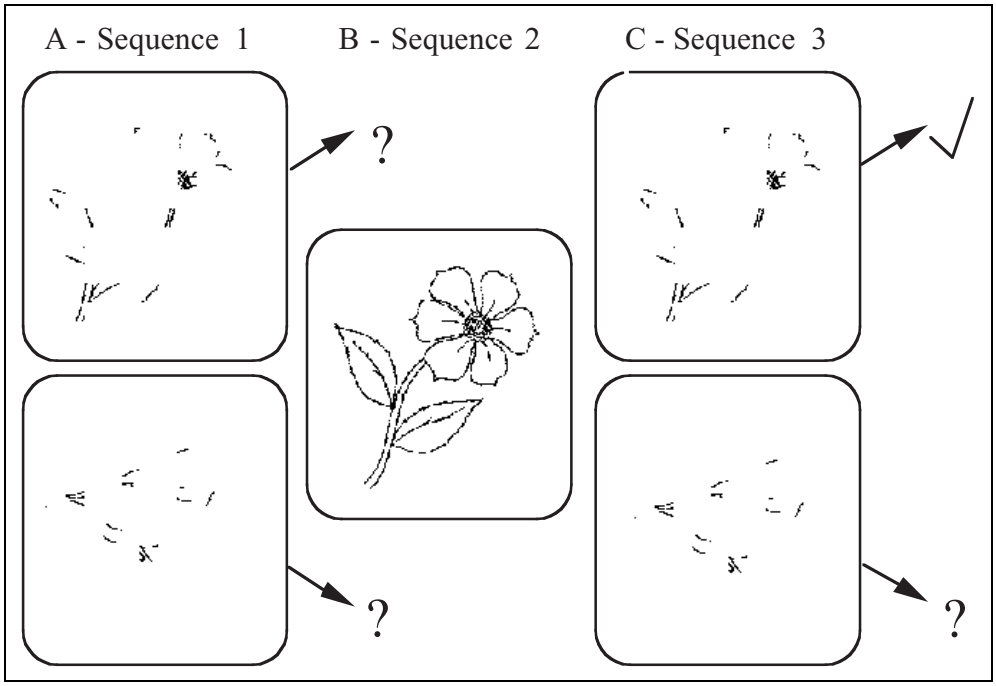

Figure 1. Schematic representation of the three sequences and stimuli used in the experiment. (A) Sequence 1 (control sequence). Subjects are unable to identify pictures. (B) Sequence 2 (presentation of 50% of unfragmented figures). (C) Sequence 3 (identification of perceptual learned objects). Pictures presented completely in Sequence 2 can be identified.

found in an associative learning task in the visual modality (Gruber et al., 2001).

As argued above, we assume that in a rapid perceptual learning task, the features of the learned object are stored in a widespread cell assembly, which possibly includes neural activity in cortical areas of both visual pathways. After learning took place, the fragmented version of a learned picture should activate the cell assembly and thus allows for the identification of that fragmented picture. To study this hypothesis, we have

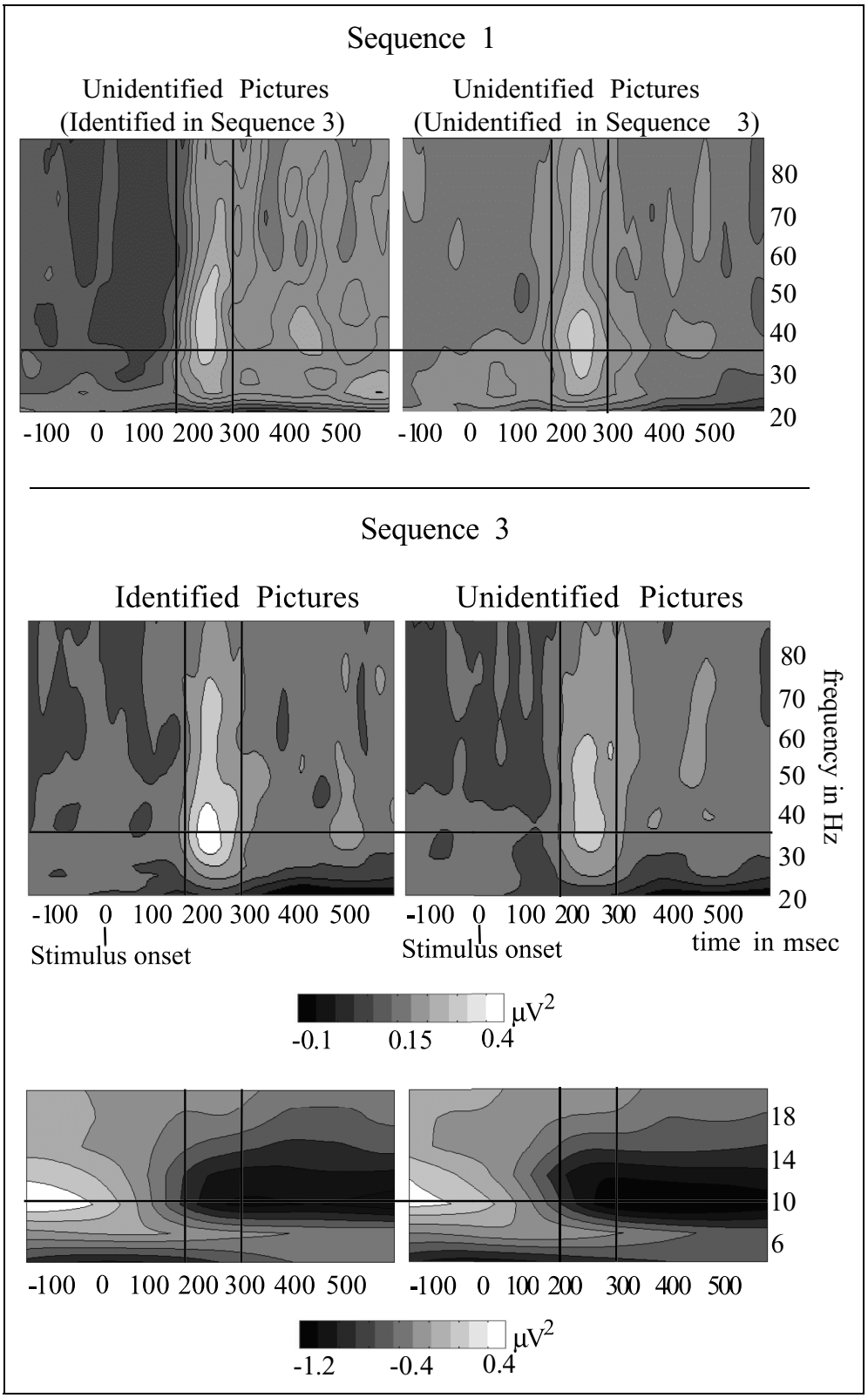

Figure 2. Grand mean baseline corrected TF plots for Sequences 1 and 3 averaged across posterior electrode sites (corresponding 10–20 positions: Cp1, Cp2, P3, Po3, Pz, Po4, P4, P7, Po7, O1, Poz, O2, Po8, P8; see Figure 6). For Sequence 3, the gamma and lower frequency range (4–20 Hz) are depicted. Note: TF plots for Sequence 1 were generated on the basis of the ratings given in Sequence 3.

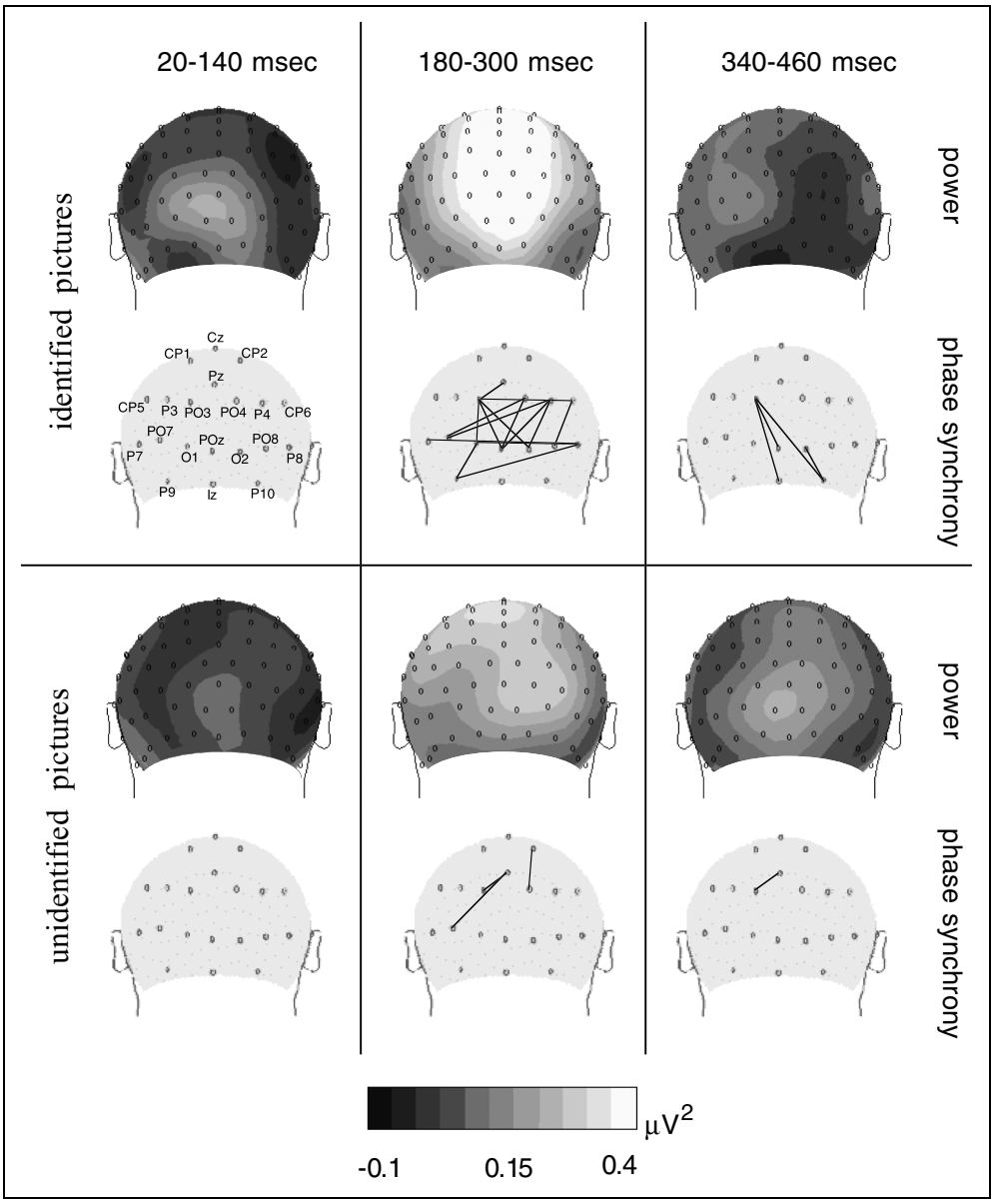

Figure 3. Upper rows: Spherical spline topographical distributions for the 36.62-Hz wavelet averaged across 9 subjects for identified and unidentified pictures after baseline correction. Lower rows: Synchronies between electrode pairs for identified and unidentified pictures. Lines are drawn only if the phase-locking value is beyond the distribution of shuffled data ($p < .01$). (A) 20–140 msec, (B) 180–300 msec, (C) 340–460 msec after stimulus onset; 10–20 locations are given in one head shape to allow for a comparison.

designed an EEG experiment using fragmented pictures from the Snodgrass and Vanderwart (1980) inventory, which could not be identified when seen in their fragmented version. However, when subjects saw the complete picture, they were easily able to identify the fragmented picture in the following sequence of the experiment (see Figure 1 for a schematic representation of the experimental design). Based on the above-discussed findings in previous EEG experiments and our hypothesis, we should find an increase in gamma power and more synchronized activity at posterior electrode sites when subjects are able to identify a fragmented figure due to prior exposure to the unfragmented version. No such pattern should be present for fragmented pictures, which subjects still cannot identify because they have never seen the complete version of that picture. In addition to analyzing the induced GBR, we examined the evoked GBR in the same frequency range as the induced GBR and the VEP. We expect no significant effects for the evoked gamma response. Due to the jitter in latency of induced responses in single epochs, we expect no significant effects in gamma power when transforming the unfiltered event-related potential (ERP) into the frequency domain (see Eckhorn, Schanze, Brosch, Salem, & Bauer, 1992 for a nice example with respect to animal data). However, it has to be mentioned that Herrmann et al. (1999) reported an increase in early-evoked GBR related to visual perception, approximately 100 msec after stimulus onset.

Furthermore, we suppose that the VEP is not optimal to detect activity in a widespread cell assembly, having the abovementioned characteristics. Thus, we expect no significant difference in the VEP in the time range of the typical occurrence of induced GBRs between 200 and 400 msec.

RESULTS

Behavioral Data

Subjects' correct identification of fragmented pictures in Sequence 3 increased significantly, when pictures were presented in their unfragmented version in Sequence 2 of the experiment. This was true for both picture sets [Pictures 1–17: $t(16) = 2.19$, $p < .05$; Pictures 18–34: $t(16) = 3.82$, $p < .01$]. Subjects' ratings after each trial were highly correlated with the correctness of picture naming after the EEG session ($\rho = .72$, $p < .0001$).

Induced Spectral Changes

Figure 2 depicts the time–frequency (TF) plots for identified and unidentified pictures in Sequences 1 and 3 of the experiment averaged across posterior electrode sites (corresponding 10–20 positions: Cp1, Cp2, P3, Po3, Pz, Po4, P4, P7, Po7, O1, Poz, O2, Po8, P8; see Figure 6). TF plots for Sequence 1 were generated on the basis of the ratings given in Sequence 3 (i.e., identified and unidentified pictures). Furthermore, the lower frequency range for Sequence 3 is depicted in separate TF plots. In Sequence 3, baseline corrected spectral power for identified pictures showed a maximum in a time window from 180 to 300 msec after stimulus onset in the frequency range of the 36.62-Hz wavelet. This maximum was significantly higher for identified as compared to unidentified pictures [$F(1,8) = 6.86$, $p < .05$]. In order to test that the increase in gamma power is a signature of rapid perceptual learning and not of the presentation of fragmented figures, we tested the 36.26-Hz wavelet for the same epoch during Sequence 1 in our experiment on the basis of the ratings given in Sequence 3. No statistically significant difference was found ($F < 1$). To consolidate these findings, the same epochs were compared between Sequences 1 and 3. The maximum of induced gamma power was significantly higher for identified pictures in Sequence 3 as compared to the same pictures in Sequence 1 [$F(1,8) = 6.29$, $p < .05$]. We found no significant differences between unidentified pictures in Sequences 1 and 3 ($F < 1$). Furthermore, induced alpha power in the time window of maximal gamma power revealed no significant differences neither for the lower (7.1–9.5 Hz) nor for the upper (9.6–12.8 Hz) alpha band ($F < 1$). The maximal alpha suppression was found in a time window from 300 to 500 msec. However, this suppression was not modulated by our experimental manipulation ($F < 1$).

In Figure 3, the grand mean spherical spline interpolated topographical distribution of the 36.26-Hz wavelet for three successive nonoverlapping time windows of 120 msec length is depicted for identified and unidentified pictures. As can be seen, if subjects were able to identify a picture, the power in the 36.26-Hz wavelet exhibited a broad posterior distribution in a time window from 180 to 300 msec, which was not present when a picture was unidentified. Post hoc t tests for posterior 10–20 electrode sites (CP1, CP2, PO3, PO4, Pz, O1, O2, Poz) revealed a significant higher gamma power for identified as compared to unidentified pictures for electrode sites: PO3 [$t(8) = 2.52$, $p < .05$], PO4 [$t(8) = 2.63$, $p < .05$], CP2 [$t(8) = 2.94$, $p < .05$], O1 [$t(8) = 3.01$, $p < .05$], POz [$t(8) = 2.68$, $p < .05$], and Pz [$t(8) = 3.75$, $p < .01$].

The highest increase in gamma power in Sequence 3 was found at electrode site Pz. Therefore, Figure 4 depicts baseline corrected mean spectral power of the time window 180–300 msec after stimulus onset at electrode Pz for the frequency ranges 17.9, 36.62, 56.15, 75.68, and 95.24 Hz (beta and gamma range). In addition, an average across the lower and upper alpha range is shown in the left panel of Figure 4. We found a significant Condition × Band interaction [$F(4,32) = 3.18$, $p < .05$]. Identified pictures are related to higher gamma power as compared to unidentified pictures only in the 36.26-Hz band [$t(8) = 3,75$, $p < 0.01$]. No such difference was found with respect to any other tested band.

Synchrony

The lower traces of Figure 3 depict phase synchrony between extended 10–20 sites for identified (upper part) and unidentified pictures (lower part) for the three time windows. Synchronies between electrode pairs are indicated by lines, which are drawn only if the synchrony value is beyond the distribution of shuffled data ($p < .01$). Practically no phase synchrony was observed for unidentified pictures in all time windows. A different picture emerged for the identified pictures in the time window of maximal power

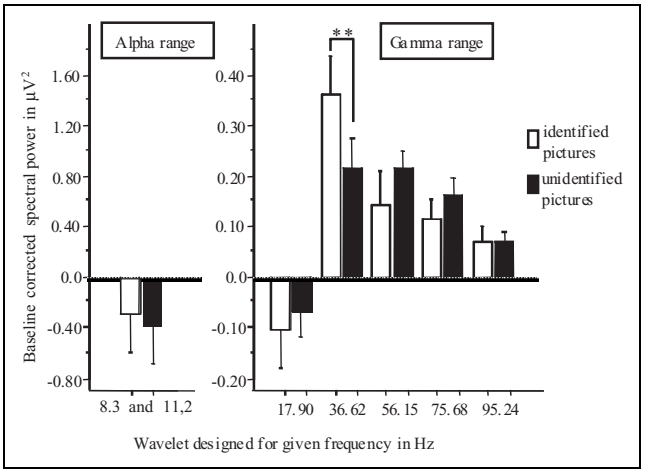

Figure 4. Spectral power across subjects for identified and unidentified pictures after baseline correction in the time window from 180 to 300 msec after stimulus onset at electrode site Pz for induced alpha, beta, and gamma band power. Note: **$p < .01$.

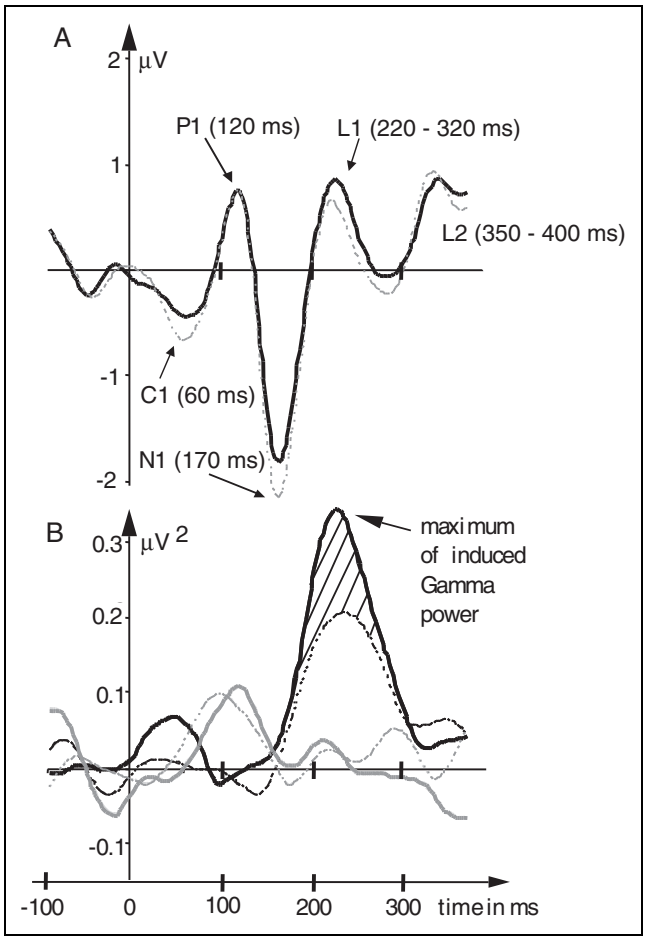

Figure 5. (A) Grand mean baseline corrected VEP for identified (solid line) and unidentified (dashed line) pictures averaged across posterior electrode sites (as in Figure 2). (B) Grand mean induced (black lines) and evoked (gray lines) gamma response for the 36.62-Hz wavelet for identified (solid lines) and unidentified (dashed lines) pictures averaged across posterior electrode sites (as in Figure 2). Statistically significant differences are indicated by diagonal lines.

amplitude. Here, significant synchronization was found for a large number of posterior electrodes, indicating synchronous neural activity in a broadly distributed posterior network.

VEP and Evoked GBR

Figure 5 depicts the grand mean VEP for identified and unidentified pictures (A) and the time course of the 36.26-Hz evoked and induced gamma band (B) averaged across posterior electrodes, respectively. Neither in the VEP nor in the 36.26-Hz evoked gamma band did we find any significant difference between identified and unidentified pictures.

DISCUSSION

The present study was designed to test the hypothesis that the identification of a fragmented picture is based on synchronized neural activity of a cell assembly acquired by rapid perceptual learning. Behavioral data verified that our experimental setup was suitable to fulfill the criteria of rapid perceptual learning. Subjects were able to identify pictures presented in their unfragmented version, but not pictures that they have not seen complete. Ratings with respect to picture identification were highly correlated to the real content of presented pictures.

We found a marked increase in induced gamma power and synchronized activity at posterior electrode sites during identification of rapid perceptually learned objects. It is unlikely that the observed effects are an artifact of processing of specific stimuli per se (i.e., a flower) because (1) no difference in induced GBRs could be observed before perceptual learning was possible and (2) the stimuli chosen for learning, that is, the unfragmented pictures, were counterbalanced across subjects. Rather, it seems plausible that the increase in spectral power and synchrony of high-frequency brain activity is related to the identification of rapid perceptually learned stimuli. This interpretation is supported by the fact that gamma activity before perceptual learning (i.e., in Sequence 1) was lower as compared to GBRs related to learned objects.

According to imaging studies, which show an increase in activity during the recall of learned objects close to the brain regions that mediate the processing of object features, multiple visual areas in the dorsal and ventral stream are assumed to be the storage sites of those features (Martin et al., 1995; Ungerleider & Haxby, 1994; Ungerleider, 1995; Roland et al., 1990). Recently, it has been proposed that such widespread cortical object representations can be regarded as Hebbian cell assemblies formed by learning processes (Gruber et al., 2001; Miltner et al., 1999; Pulvermüller, 1996) and that neuronal activity within and between the elements of such a network is integrated by synchronization in the gamma range, that is, frequencies >20 Hz (Hummel & Biederman, 1992; Eckhorn et al., 1990; Singer et al., 1990; Singer & Gray, 1995; Gray et al., 1989, 1990; Malsburg & Schneider, 1986; Milner, 1974). A number of studies have reliably shown that induced GBRs can be measured in human EEG (Gruber et al., 1999; Keil et al., 1999; Rodriguez et al., 1999; Tallon-Baudry, Bertrand, Delpuech, et al., 1997; Tallon-Baudry, Bertrand, Wienbruch, et al., 1997; Müller et al., 1996, 1997, 2000; Lutzenberger et al., 1995). A common feature in these studies is the main activity in a latency range between 200 and 400 msec (see also Keil, Gruber, & Müller, 2001; Tallon-Baudry & Bertrand, 1999). Our present results match the latency range of previous findings. Therefore, one can exclude that early feed-forward mechanisms account for the increase in induced GBR in our and others findings. Rather, we see induced GBRs in the present case as a signature of cortical object representations established by synchronized neural activity of a

distributed cell assembly. This hypothesis is supported by theoretical assumptions on object identification. For instance, Hummel & Biederman (1992) proposed that their so-called ''geons'' are established by the synchronization of oscillatory outputs of units representing features of one ''geon.'' Grossberg (1995) proposed in his ''adaptive resonance'' theory that spatially distributed features are linked to an object by means of synchronous oscillations. After learning took place, the fragmented version of a previously seen unfragmented picture possibly activates its cortical representation and thus allows for the identification of the fragmented picture. Furthermore, we assume that the integration of activity in the dorsal and ventral pathway of visual information processing might have contributed to the increase in power and phase synchrony, but this is speculative at present. However, an increase in activity in these areas was reported in human imaging and animal studies. In an experiment using human positron emission tomography (PET), Dolan et al. (1997) found an increase in activity in parietal and temporal areas after rapid perceptual learning. Tovee, Rolls, and Ramachandran (1996) reported an increase in neuron's firing rate using a rapid perceptual learning paradigm in temporal cortical visual areas in macaques. In a visual pattern memory study using PET, Roland et al. (1990) reported an increase in activity in parieto-occipital areas during recall of stimuli. Such findings support our hypothesis that multiple posterior areas have contributed to our results.

The pattern of phase synchrony between electrode sites fits the maximum induced GBR spectral power well, both with respect to the topographical distribution and the time course of the activity. Thus, an increase in spectral power is closely linked to an increase in phase synchrony. It is important to mention that phase synchrony at the scalp surface cannot totally rule out the contribution of a single neural source located at a distance from two testing electrodes, which may create an artificial synchronization of EEG signals by simple volume conduction. However, Lachaux et al. (1999) stated that volume conduction leads to a diffusion in the measurement of synchrony. This would mean that values of synchrony are centered around a maximum at the scalp surface and get weaker with more distance from that maximum. We did not find such diffusion, rather synchrony between distant electrode sites, but not between electrode sites located between the two. Yet, it has to be mentioned that this rule of thumb is not a reliable test to identify conduction synchronies and cannot provide a complete solution to the problem. Furthermore, another problem in calculating synchrony is not only volume conduction but also the choice of an appropriate reference electrode. Lachaux et al. (1999) showed that the calculation of current source density can create artificial synchrony. An alternative approach is to use the average reference. Although this method does not completely solve the problem, we adopted this strategy for our experiment.

An interesting point is that we neither found a significant enhancement of gamma power at frontal electrode sites nor any significant phase locking from posterior to frontal electrode sites. We assume this is due to the more implicit nature of our task, that is, the facilitation of performance without intentional recollection (Schacter, 1987). A similar lack of prefrontal activation was reported by Klingberg and Roland (1998) in an associative learning task. These authors speculated that the prefrontal cortex is not activated when retrieval is automatic.

Interestingly, the induced alpha suppression that we found in Sequence 3 shows a similar pattern as a process commonly referred to as event-related desynchronization (Pfurtscheller & Lopes da Silva, 1999). In a number of studies, changes in event-related alpha power have been linked to memory processes (Klimesch, 1996, 1999). The fact that we found no differences between identified and unidentified pictures neither in the lower nor in the upper alpha band leads us to the conclusion that the induced alpha decrease in our study may play a functionally different role in perceptual learning as compared to induced GBRs. However, due to the fact that our study mainly aimed on the investigation of induced frequency synchronization, the interpretation of lower frequency desynchronization goes beyond the aims of our study and should be subject of follow-up experiments.

We found no significant differences between identified and unidentified pictures for the 36.62-Hz evoked GBR and the VEP. With respect to the evoked gamma response, we assume that due to the jitter in the latency of induced responses in single epochs, these responses are averaged out in the evoked spectrum (Eckhorn et al., 1990). In accordance with other studies (Herrmann et al., 1999; Tallon et al., 1995), we found an increase in the evoked gamma response around 110 msec after stimulus onset. However, this increase was not significantly different from baseline and showed no significant condition effect. It might be the case that low-level processing in early visual areas is reflected by evoked GBRs in the human EEG, which might be complementary to VEPs. However, the fact that we found no significant relation of induced GBRs to the evoked GBR indicates that evoked responses may play a functionally different role in perceptual learning as compared to induced high-frequency responses.

In line with EEG studies examining the identification of fragmented pictures (Doniger et al., 2000; Viggiano & Kutas, 2000), we found no difference between identified and unidentified pictures for the P1 and N1 VEP component, respectively. Furthermore, we found no significant difference in the VEP in the time range of the occurrence of induced GBRs. We conclude that the visual evoked response is suboptimal to uncover neural

activity distributed over a number of cortical areas forming a Hebbian-like cell assembly, which we presume as the underlying mechanism for rapid perceptual learning. Although Viggiano and Kutas (2000) reported a difference between identified and unidentified pictures in a late evoked component, this modulation appeared in a time range after the modulation of our induced gamma band modulation. Due to the setting of the time constant of our EEG amplifier in the present recording, we were unable to analyze evoked potential components later than 400 msec. Doniger et al. (2000) reported a visual evoked component "N_{cl}" peaking 290 msec after stimulus onset, which is possibly related to "perceptual closure" processes. However, this study used a different experimental paradigm, namely stepwise presentation of decreasing fragmentation levels until identification. Thus, a direct comparison to our rapid perceptual learning task is problematic. Although the evoked response in our study showed a similar time course as compared to their results, we assume that we have not found a modulation in the time window of the "N_{cl}" component because fragmentation levels in our study were higher as compared to Doniger et al.'s work. Very importantly, induced responses in the gamma range were modulated before the time window of the "N_{cl}". This fits well Doniger et al.'s reasoning that a cortical object representation must be established before "perceptual closure" can take place. In line with Doniger et al., Stuss, Picton, Cerri, Leech, and Stethem (1992) reported a negative EP component in a similar time window. Furthermore, Stuss et al. found a late positive wave 550–650 msec after stimulus onset for correctly identified pictures, which might be a signature of the subject's certainty about perceptual analysis and may therefore reflect a subsequent step in the processing of fragmented pictures.

In summary, the present experiment has several implications for the understanding of neural mechanism of perceptual learning. Induced GBRs and phase synchrony may be a signature of cortical object representation stored in a Hebbian cell assembly, which is crucial for the identification of a fragmented picture in a rapid perceptual learning task. Such a cell assembly has to integrate neural activity from different visual cortices processing different features of a stimulus. The fact that we found no significant effects with respect to the evoked GBR and the VEP points out that evoked responses may play a functionally different role in perception as compared to induced GBRs.

METHODS

Subjects

Twelve healthy, right-handed university students (7 men, 5 women) received class credits or a small financial bonus for participation. Their age ranged from 21 to 27 (mean: 25.0 years, *SD* 2.04 years). All had normal or corrected-to-normal visual acuity. Informed consent was obtained from each participant.

Stimuli and Task

Stimuli were 34 line drawings taken from the Snodgrass and Vanderwart (1980) inventory both in their complete and incomplete version. Fragmentation level was chosen to meet the requirements for rapid perceptual learning, that is, drawings could not be identified when presented for the first time but can easily be named once presented in their unfragmented version. Stimuli were centrally presented on a computer screen placed 1.5 m in front of the subjects with a frame rate of 70 Hz. A white fixation square of $0.3^\circ \times 0.3^\circ$ of visual angle was always present in the center of the screen. The line drawings—covering a visual angle of approximately $4.5^\circ \times 5.2^\circ$—were presented in white on a black background. In preexperimental test trials, we presented all 34 pictures in their fragmented version to exclude drawings that subjects were able to identify without presentation of the respective unfragmented version.

The experimental design comprised three sequences (see Figure 1). In Sequence 1, all pictures were presented with a level of fragmentation such that subjects were unable to identify them (control sequence—see Figure 1A). Each stimulus was presented five times in randomized order. Thus, 170 trials were presented in Sequence 1, each consisted of a 500-msec baseline period (black screen), a 700-msec picture presentation time, and an interstimulus interval between 700 and 1200 msec. Picture onset was synchronized to the vertical retrace of the monitor. In Sequence 2, one half of the pictures were presented in their unfragmented version (rapid perceptual learning sequence—see Figure 1B). To control for effects related to drawing's contents per se, one half of the subjects were shown complete versions of Pictures 1–17, the other half of subjects saw complete versions of Pictures 18–34. The time course of one trial was equivalent to that of Sequence 1. Again, each picture was presented five times in randomized order, that is, 85 trials were represented. In Sequence 3, all pictures were displayed again in their fragmented version (recognition of perceptual learned objects—see Figure 1C). Again, the time course of one trial and the number of presentations were identical to that of Sequence 1. After each trial, subjects had to rate how sure they were with respect to the identification of the picture via the numeric keyboard on a scale from 0 to 3 (0 = *very sure*, 1 = *sure*, 2 = *not sure*, 3 = *not at all*). The next trial started with a delay of 500 msec after subject's response. This delay was introduced in order to avoid the contamination of the post motor potential during the following 500-msec black screen baseline period (Neshige, Luders, & Shibasaki, 1988). Subjects were instructed to avoid eye

movements and blinks while attending the pictures and to maintain their gaze to the fixation square in the middle of the screen. Two experimental conditions were defined on the basis of this experimental design (''identified pictures,'' i.e., rating 0 or 1, and ''unidentified pictures,'' i.e., rating 2 or 3). To control the ranking with respect to the correctness of subjects' ratings, they named the objects on pictures rated with 0 or 1 in Sequence 3 after the EEG session. Correct and incorrect answers were documented.

Electrophysiological Recordings

EEG was recorded continuously with an EGI (Electrical Geodesics Inc.) 128-electrode array. A schematic representation of the electrode array and corresponding extended international 10–20 electrode sites is given in Figure 6. The vertex (recording site Cz) was chosen as reference. As suggested for the EGI high input impedance amplifier, impedances were kept below 50 kΩ. Sampling rate was 500 Hz, and all channels were preprocessed on-line by means of 0.1- to 200-Hz band-pass filter. In addition, vertical and horizontal eye movements were monitored with a subset of the 128 electrodes. Further data processing was performed off-line.

Data Reduction and Analysis

EEG was segmented to obtain epochs containing 500 msec prior and 1500 msec following stimulus onset. Artifact correction was performed by means of the ''statistical correction of artifacts in dense array studies'' (SCADS) procedure developed by Junghöfer, Elbert, Tucker, and Rockstroh (2000). This procedure uses a combination of trial exclusion and channel approximation based on statistical parameters of the data. In the first step, recording channel artifacts are detected using the recording reference (Cz). Subsequently, global artifacts are detected using the average reference. In the next interactive step, distinct sensors from particular trials are removed on the basis of the distribution of their amplitude, standard deviation, and gradient. The information of eliminated electrodes is replaced with a statistically weighted spherical interpolation from the full channel set. Lastly, the variance of the signal across trials is computed to document the stability of the average waveform. The limit for the number of approximated channels was set to 20 channels. With respect to the spatial arrangement of the approximated sensors, it was ensured that the rejected sensors are not located within one region of the scalp, because this would make interpolation for this area invalid. Single epochs with excessive eye movements and blinks or more than 20 channels containing artifacts were discarded. Using this method, 3 subjects were excluded due to excessive artifacts. For the remaining 9 subjects, the average rejection rate was 30%. For further analysis, the average reference was used.

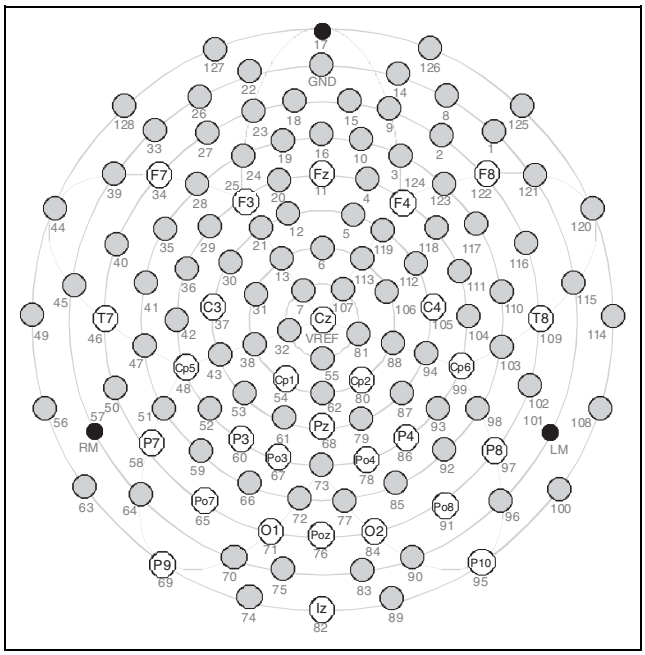

Figure 6. Schematic representation of a 128-channel montage. Extended 10–20 sites are given to allow for a comparison. Note: 10–20 sites to the closest electrode in the net.

Data Analysis: Behavioral Data

To analyze the difference in identification between pictures presented completely in Sequence 2 and the ones not shown completely, the number of correct answers in the former was compared with the number of correct answers in the latter by means of paired *t* tests over the range of items. This was done separately for subjects who have seen Pictures 1–17 or 18–34 completely. Furthermore, a Spearman rank correlation between subject's ratings from 0 to 3 and the correctness of picture naming were calculated.

Data Analysis: Induced Spectral Changes

A given EEG epoch can be modeled by the sum of the evoked response plus the trial-by-trial fluctuation around the mean (Priestley, 1988). Since the present analysis focused on non-phase-locked oscillatory activity, the evoked response (i.e., the VEP) was subtracted from each trial (see also Müller et al., 1996 for a similar procedure). Using a wavelet analysis of the artifact-free epochs, spectral changes in gamma band oscillatory activity during Sequences 1 and 3 were analyzed. In particular, complex Morlet wavelets were used for frequency analysis to overcome certain problems with constant Fast Fourier Transform window length. This method provides a good compromise between time and

frequency resolution (Sinkkonen, Tiitinen, & Naatanen, 1995), in particular, time resolution of this procedure increases with frequency, whereas frequency resolution decreases. Thus, this technique is especially suited for detecting induced high-frequency oscillations that may occur during brief periods. The present procedure has been proposed by Bertrand and Pantev (1994) and is described in detail elsewhere, for example, by Tallon-Baudry, Bertrand, Delpuech, et al. (1997) and Tallon-Baudry et al. (1998). In brief, the method provides a time-varying magnitude of the signal in each frequency band, leading to time by frequency (TF) representation of the signal. TF energy is averaged across single trials, allowing one to analyze non-phase-locked high-frequency components. To that end, complex Morlet wavelets, g, can be generated in the time domain for different analysis frequencies, f_0, according to

$$g(t,f_0) = A' e^{-\frac{t^2}{2\sigma_t^2}} e^{2i\pi f_0 t} \quad (1)$$

with A' depending on the parameter σ_f, specifying the width of the wavelet in the frequency domain, the analysis frequency, f_0, and the user-selected ratio, m:

$$A' = \sigma_f \sqrt{2\pi^3} \sqrt{\frac{m}{f_0\sqrt{\pi}}} \quad (2)$$

with

$$m = \frac{f_0}{\sigma_f} \quad (3)$$

Thus, given a constant ratio m, the width of the wavelets in the frequency domain, σ_f, changes as a function of the analysis frequency, f_0. In order to achieve good time and frequency resolution, the wavelet family that we used is defined by a constant $m = f_0/\sigma_f = 7$ with f_0 ranging from 8.37 to 96.04 Hz in 0.49-Hz steps. Wavelets of this family were normalized in order to have equal amounts of energy. For each epoch, the time-varying energy in a given frequency band was calculated, this being the absolute value of the convolution of the signal with the wavelet for each epoch and each complex spectrum. An epoch from 400 to 100 msec prior to stimulus onset was used as an estimate of general noise. The mean of this baseline epoch was subtracted from the TF matrix for each frequency and time point for each electrode, respectively. After wavelet analysis, mean spectral power in Sequences 1 and 3 of the experiment averaged across posterior electrode sites (corresponding 10–20 positions: Cp1, Cp2, P3, Po3, Pz, Po4, P4, P7, Po7, O1, Poz, O2, Po8, P8; see Figure 6) was represented in TF plots for the gamma range for identified pictures (rating 0 and 1) and unidentified pictures (rating 2 and 3). TF plots for Sequence 1 were generated on the basis of the ratings given in Sequence 3. Electrode sites used for these TF plots were selected on the basis of previous findings regarding visual information processing (Tallon-Baudry & Bertrand, 1999). Furthermore, for Sequence 3, the lower frequency range is depicted in separate TF plots (4–20 Hz). The TF plots were used to identify the time window and frequency band showing maximal spectral power. For further statistical analysis, the identified time window and frequency band were utilized. A repeated-measures ANOVA with the factors Condition (identified vs. unidentified pictures) and Recording Site (29 electrodes) was used to calculate for electrode sites corresponding to the extended international 10–20 system (see Figure 6). To make sure that our findings show an effect of perceptual learning, a Condition (identified vs. unidentified pictures) × Recording Site (29 electrodes) repeated-measures ANOVA was performed for epochs recorded in Sequence 1, that is, before perceptual learning has taken place. In particular, epochs from Sequence 1 were grouped according to the subjects' ratings in Sequence 3. Obviously, we did not expect any differences here. To consolidate our results, the same ANOVA models were applied to compare Sequences 1 and 3. In particular, we compared identified and unidentified pictures in Sequence 3 to matched epochs in Sequence 1. Furthermore, induced alpha power in Sequence 3 was analyzed for a wavelet designed for the lower (8.3 Hz) and the upper (11.2 Hz) alpha band. Time windows in the alpha range were chosen according to the maximum of induced gamma power. Furthermore, a time window showing maximal alpha suppression was analyzed.

Post hoc comparisons were evaluated by means of paired t tests for 10–20 electrode sites showing maximal spectral power. To control for effects in other high-frequency bands, the electrode showing maximal spectral power in the first step of analysis was inspected by means of a Condition (identified vs. unidentified) × Band (17.9 Hz, 36.62 Hz, 56.15 Hz, 75.68 Hz, 95.24 Hz) repeated-measures ANOVA.

Topographies of spectral power of the 36.62-Hz wavelet for succeeding nonoverlapping time windows after stimulus onset were calculated with an algorithm developed by Junghöfer, Elbert, Leiderer, Berg, and Rockstroh (1997), which uses spherical spline interpolations using all 128 electrodes.

Data Analysis: Synchrony

Phase synchrony analysis was performed, elaborating on a procedure suggested by Rodriguez et al. (1999), which provides a method of measuring synchronous oscillatory activity independent of the signal's amplitude. For each subject, phase synchrony was computed for a distinct frequency, f_0, of his/her maximal gamma activity. Phase is measured by convoluting the signal with a complex Morlet wavelet designed for f_0

(see above). A complex phase value ρ is then computed at frequency f_0, for each electrode, each time bin, and each trial by dividing the result of the convolution by the magnitude of this result. According to Rodriguez et al. subsequently, a phase-locking value is computed as:

$$\rho_{ij} = \frac{|\sum \rho_i - \rho_j|}{N} \quad (4)$$

where N is the number of trials, and i and j are the indices for the pair of electrodes to be compared. For the sake of data reduction, phase-locking values were computed only for a subset of the 128-channel set, corresponding to electrode sites of the extended 10–20 system. ρ_{ij} results in a real value between 1 (constant phase differences) and 0 (random phase differences). These values were normalized by subtracting the mean value of the baseline period (black screen; 400–100 msec before stimulus onset) and were divided by the standard deviation of this time window. To provide a topographical representation of phase-locking values over individual pairs of electrodes in a distinct time window, a statistical randomization technique was used. Time windows were chosen, which were the same as those in the analysis of induced GBRs. Averaged phase synchronies for these time windows (W_{ij}) between electrodes i and j were calculated. For each of these averages, 200 values were analogously computed on shuffled data. Shuffling is done by calculating synchronies over time windows not phase locked to stimulus onset. The average W_{ij} was retained as statistically significant if it was greater than the maximum of the 200 shuffled values, thus indicating a two-tailed probability value of $p = .01$. On a topographical template of the electrode layout, any significant value W_{ij} is indicated by a line from electrode i to electrode j.

Data Analysis: VEP and Evoked GBR

Visual Evoked Potential

A 20-Hz low-pass filter was applied to the data before all ERP analyses. Baseline correction was performed by subtracting the mean of the signal during the time window from 400 to 100 msec prior to stimulus onset. Five ERP components were defined on the basis of overall root mean square (RMS) amplitude: C1 (40–80 msec), P1 (100–140 msec), N1 (150–190 msec), a first late component L1 (220–320 msec), and a second late component L2 (350–400 msec). Due to the time constant of the used 0.1 on-line filter, no later EP components were analyzed. Amplitudes were averaged across the defined time windows. Mean amplitudes at electrode sites corresponding to the extended international 10–20 system were analyzed using a Condition (identified vs. unidentified) × Recording Site (29 electrodes) repeated-measures ANOVA for each of the described components. Post hoc comparisons were calculated by means of paired t tests.

Evoked GBR

Evoked GBRs were extracted by applying the above-described wavelet analysis to the unfiltered averaged evoked response. To allow for a comparison between induced and evoked gamma activity, we applied the same ANOVA models as for induced GBRs to evoked spectral changes. Due to the fact that we have found no obvious peak in the evoked TF representations of the two experimental conditions, we used the same frequency bands as for induced GBRs for statistical analysis.

Where appropriate, p values were adjusted by Greenhouse–Geisser correction in all ANOVA models. Post hoc t tests were Bonferroni corrected. Means and standard errors are presented.

Acknowledgments

We are grateful to Heidi Messmer for her help in data acquisition. This research was supported by the Deutsche Forschungsgemeinschaft.

Reprint requests should be sent to Thomas Gruber, Cognitive Neuroscience, Department of Psychology, University of Liverpool, Eleanor Rathbone Building, Bedford Street South, Liverpool, L69 7ZA, UK, or via e-mail: tgruber@liverpool.ac.uk.

REFERENCES

Bertrand, O., & Pantev, C. (1994). Stimulus frequency dependence of the transient oscillatory auditory evoked response (40 Hz) studied by electric and magnetic recordings in human. In C. Pantev, T. Elbert, & B. Lütkenhöner (Eds.), *Oscillatory event-related brain dynamics* (pp. 231–242). New York: Plenum.

Biederman, I. (1987). Recognition-by-components: A theory of human image understanding. *Psychological Review, 94,* 115–147.

Dolan, R. J., Fink, G. R., Rolls, E., Booth, M., Holmes, A., Frackowiak, R. S., & Friston, K. J. (1997). How the brain learns to see objects and faces in an impoverished context. *Nature, 389,* 596–599.

Doniger, G. M., Foxe, J. J., Murray, M. M., Higgins, B. A., Snodgrass, J. G., & Schroeder, C. E. (2000). Activation timecourse of ventral visual stream object-recognition areas: High density electrical mapping of perceptual closure processes. *Journal of Cognitive Neuroscience, 12,* 615–621.

Eckhorn, R., Reitboeck, H. J., Arndt, M., & Dicke, P. (1990). Feature linking via synchronization among distributed assemblies: Simulations of results from cat visual cortex. *Neural Computation, 2,* 293–307.

Eckhorn, R., Schanze, T., Brosch, M., Salem, W., & Bauer, R. (1992). Stimulus-specific synchronizations in cat visual cortex: Multiple microelectrode and correlation studies from several cortical areas. In E. Basar & T. H. Bullock (Eds.), *Induced rhythms in the brain* (pp. 47–82). Boston: Birkhäuser.

Felleman, D. J., & van Essen, D. C. (1991). Distributed

hierarchical processing in the primate cerebral cortex. *Cerebral Cortex, 1,* 1–47.
Gomez-Gonzales, C. M., Clark, V. P., Fan, S., Luck, S. J., & Hillyard, S. A. (1994). Sources of attention-sensitive visual event-related potentials. *Brain Topography, 7,* 41–51.
Gray, C. M., Engel, A. K., König, P., & Singer, W. (1990). Stimulus-dependent neuronal oscillations in cat visual cortex: Receptive field properties and feature dependence. *European Journal of Neuroscience, 2,* 607–619.
Gray, C. M., König, P., Engel, A. K., & Singer, W. (1989). Oscillatory responses in cat visual cortex exhibit inter-columnar synchronization which reflects global stimulus properties. *Nature, 338,* 334–337.
Grossberg, S. (1995). The attentive brain. *American Scientist, 83,* 438–449.
Gruber, T., Keil, A., & Müller, M. M. (2001). Modulation of induced gamma band responses and phase synchrony in an associative learning task in the human EEG. *Neuroscience Letters, 316,* 29–32.
Gruber, T., Müller, M. M., Keil, A., & Elbert, T. (1999). Selective visual-spatial attention alters induced gamma band responses in the human EEG. *Clinical Neurophysiology, 110,* 2074–2085.
Hebb, D. O. (1949). *The organization of behavior.* Chichester, UK: Wiley.
Herrmann, S., Mecklinger, A., & Pfeifer, E. (1999). Gamma responses and ERPs in a visual classification task. *Clinical Neurophysiology, 110,* 636–642.
Hummel, J. E., & Biederman, I. (1992). Dynamic binding in a neural network for shape recognition. *Psychological Review, 99,* 480–517.
Humphrey, G. W., & Bruce, V. (1989). *Visual cognition: Computational, experimental and neuropsychological perspectives.* Hillsdale, NJ: Erlbaum.
Junghöfer, M., Elbert, T., Leiderer, P., Berg , P., & Rockstroh, B. (1997). Mapping EEG-potentials on the surface of the brain: A strategy for uncovering cortical sources. *Brain Topography, 9,* 203–217.
Junghöfer, M., Elbert, T., Tucker, D. M., & Rockstroh, B. (2000). Statistical control of artifacts in dense array EEG/MEG studies. *Psychophysiology, 37,* 523–532.
Keil, A., Gruber, T., & Müller, M. M. (2001). Functional correlates of macroscopic high-frequency brain activity in the human visual system. *Neuroscience and Biobehavioral Reviews, 25,* 527–534.
Keil, A., Müller, M. M., Ray, W. J., Gruber, T., & Elbert, T. (1999). Human gamma band activity and perception of a gestalt. *Journal of Neuroscience, 19,* 7152–7161.
Klimesch, W. (1996). Memory processes, brain oscillations and EEG synchronization. *International Journal of Psychophysiology, 24,* 61–100.
Klimesch, W. (1999). EEG alpha and theta oscillations reflect cognitive and memory performance: A review and analysis. *Brain Research Reviews, 29,* 169–195.
Klingberg, T., & Roland, P. E. (1998). Right prefrontal activation during encoding, but not during retrieval, in a non-verbal paired-associates task. *Cerebral Cortex, 8,* 73–79.
Lachaux, J. P., Rodriguez, E., Martinerie, J., & Varela, F. J. (1999). Measuring phase synchrony in brain signals. *Human Brain Mapping, 8,* 194–208.
Leeper, R. (1935). A study of a neglected portion of the field of learning. The development of sensory organization. *Journal of Genetic Psychology, 46,* 41–75.
Livingstone, M., & Hubel, D. (1988). Segregation of form, color, movement, and depth: Anatomy, physiology, and perception. *Science, 240,* 740–749.
Lutzenberger, W., Pulvermüller, F., Elbert, T., & Birbaumer, N. (1995). Visual stimulation alters local 40-Hz responses in humans: An EEG-study. *Neuroscience Letters, 183,* 39–42.
Malsburg, C. V. D., & Schneider, W. (1986). A neural cocktail-party processor. *Biological Cybernetics, 54,* 29–40.
Martin, A., Haxby, J. V., Lalonde, F. M., Wiggs, C. L., & Ungerleider, L. G. (1995). Discrete cortical regions associated with knowledge of color and knowledge of action. *Science, 270,* 102–105.
Milner, P. M. (1974). A model for visual shape recognition. *Psychological Review, 81,* 521–535.
Miltner, W. H. R., Braun, C., Arnold, M., Witte, H., & Taub, E. (1999). Coherence of gamma-band activity as a basis for associative learning. *Nature, 397,* 434–436.
Müller, M. M., Bosch, J., Elbert, T., Kreiter, A., Valdes Sosa, M., Valdes Sosa, P., & Rockstroh, B. (1996). Visually induced gamma-band responses in human electroencephalographic activity—a link to animal studies. *Experimental Brain Research, 112,* 96–102.
Müller, M. M., & Gruber, T. (2001). Induced gamma-band responses in the human EEG are related to attentional information processing. *Visual Cognition, 8,* 579–592.
Müller, M. M., Gruber, T., & Keil, A. (2000). Modulation of induced gamma band activity in the human EEG by attention and visual information processing. *International Journal of Psychophysiology, 38,* 283–299.
Müller, M. M., Junghöfer, M., Elbert, T., & Rockstroh, B. (1997). Visually induced gamma-band responses to coherent and incoherent motion: A replication study. *NeuroReport, 8,* 2575–2579.
Neshige, R., Luders, H., & Shibasaki, H. (1988). Recording of movement-related potentials from scalp and cortex in man. *Brain, 111,* 719–736.
Pfurtscheller, G., & Lopes da Silva, F. H. (1999). Event-related EEG/MEG synchronization and desynchronization: Basic principles. *Clinical Neurophysiology, 110,* 1842–1857.
Priestley, M. B. (1988). *Non-linear and non-stationary time series analysis.* London: Academic Press.
Pulvermüller, F. (1996). Hebb's concept of cell assemblies and the psychophysiology of word processing. *Psychophysiology, 33,* 317–333.
Ramachandran, V. S. (1994). 2-D or not 2-D—that is the question. In R. Gregory, J. Harris, P. Heard, & D. Rose (Eds.), *The artful eye* (pp. 249–267). Oxford, UK: Oxford University Press.
Rodriguez, E., George, N., Lachaux, J. P., Martinerie, J., Renault, B., & Varela, F. J. (1999). Perception's shadow: Long-distance synchronization of human brain activity. *Nature, 397,* 430–433.
Roland, P. E., Gulyas, B., Seitz, R. J., Bohm, C., Stone-Elander, S. (1990). Functional anatomy of storage, recall, and recognition of a visual pattern in man. *NeuroReport, 1,* 53–56.
Schacter, D. L. (1987). Implicit memory: History and current status. *Journal of Experimental Psychology. Learning, Memory and Cognition, 13,* 501–518.
Schacter, D. L. (1992). Understanding implicit memory: A cognitive neuroscience approach. *American Psychologist, 47,* 559–569.
Schacter, D. L., Bowers, J., & Booker, J. (1989). *Intention, awareness, and implicit memory: The retrieval intentionality criterion.* Hillsdale, NJ: Erlbaum.
Singer, W., Gray, C., Engel, A., König, P., Artola, A., & Bröcher, S. (1990). Formation of cortical cell assemblies. *Cold Spring Harbor Symposia on Quantitative Biology, 55,* 939–952.
Singer, W., & Gray, C. M. (1995). Visual feature integration and the temporal correlation hypothesis. *Annual Review of Neuroscience, 18,* 555–586.

Sinkkonen, J., Tiitinen, H., & Näätänen, R. (1995). Gabor filters: An informative way for analysing event-related brain activity. *Journal of Neuroscience Methods, 56,* 99–104.

Snodgrass, J. G., & Vanderwart, M. (1980). A standardized Set of 260 pictures: Norms for name agreement, image agreement, familiarity and visual complexity. *Journal of Experimental Psychology. Human Learning and Memory, 6,* 174–215.

Stuss, D. T., Picton, T. W., Cerri, A. M., Leech, E. E., & Stethem, L. L. (1992). Perceptual closure and object identification: Electrophysiological responses to incomplete pictures. *Brain and Cognition, 19,* 253–266.

Tallon, C., Bertrand, O., Bouchet, P., & Pernier, J. (1995). Gamma-range activity evoked by coherent visual stimuli in humans. *European Journal of Neuroscience, 7,* 1285–1291.

Tallon-Baudry, C., & Bertrand, O. (1999). Oscillatory gamma activity in humans and its role in object representation. *Trends in Cognitive Sciences, 3,* 151–162.

Tallon-Baudry, C., Bertrand, O., Delpuech, C., & Pernier, J. (1997). Oscillatory gamma-band (30–70 Hz) activity induced by a visual search task in human. *Journal of Neuroscience, 17,* 722–734.

Tallon-Baudry, C., Bertrand, O., Peronnet, F., & Pernier, J. (1998). Induced gamma-band activity during the delay of a visual short-term memory task in humans. *Journal of Neuroscience, 18,* 4244–4254.

Tallon-Baudry, C., Bertrand, O., Wienbruch, C., Ross, B., & Pantev, C. (1997). Combined EEG and MEG recordings of visual 40-Hz responses to illusory triangles in human. *NeuroReport, 8,* 1103–1107.

Tootell, R. B., Dale, A. M., Sereno, M. I., & Malach, R. (1996). New images from human visual cortex. *Trends in Neuroscience, 19,* 481–489.

Tovee, M. J., Rolls, E. T., & Ramachandran, V. S. (1996). Rapid visual learning in neurones of the primate temporal visual cortex. *NeuroReport, 7,* 2757–2760.

Treisman, A. (1988). Features and objects. *Quarterly Journal of Experimental Psychology, 40,* 201–237.

Treisman, A. (1992). Perceiving and re-perceiving objects. *American Psychologist, 47,* 862–875.

Ungerleider, L. G. (1995). Functional brain imaging studies of cortical mechanisms for memory. *Science, 270,* 769–775.

Ungerleider, L. G., & Haxby, J. V. (1994). 'What' and 'where' in the human brain. *Current Opinion in Neurobiology, 4,* 157–165.

Viggiano, M. P., & Kutas, M. (2000). Overt and covert identification of fragmented objects inferred from performance and electrophysiological measures. *Journal of Experimental Psychology, General, 129,* 107–125.

Warren, C. E. J., & Morton, J. (1982). The effects of priming in picture recognition. *British Journal of Psychology, 73,* 117–130.

Zeki, S. (1993). *A vision of the brain* (1st ed.). Oxford, UK: Basil Blackwell.